Nanomechanical analysis of bone tissue engineering scaffolds

Jessica D. Kaufman,[1] Jie Song,[2,3] Catherine M. Klapperich[4,1]
[1]*Department of Biomedical Engineering, Boston University, Boston, Massachusetts 02215*
[2]*Materials Sciences Division, Lawrence Berkeley National Laboratory, University of California, Berkeley, California 94720*
[3]*The Molecular Foundry, Lawrence Berkeley National Laboratory, University of California, Berkeley, California 94720*
[4]*Department of Manufacturing Engineering, Boston University, Boston, Massachusetts 02215*

Received 17 August 2005; revised 9 June 2006; accepted 26 June 2006
Published online 22 December 2006 in Wiley InterScience (www.interscience.wiley.com). DOI: 10.1002/jbm.a.30976

Abstract: Copolymers of (2-hydroxyethyl methacrylate) (HEMA) and methacrylamide monomers conjugated with amino acids were synthesized and crosslinked with ethylene glycol dimethacrylate. The resulting library of copolymers was mineralized *in vitro* using two distinct methods. In the first mineralization method, the copolymers were polymerized in the presence of a sub-micron hydroxyapatite (HA) suspension. In the second method, copolymers were mineralized with HA using a urea-mediated process. The mechanical properties of all of the copolymers, both mineralized and not, were determined using nanoindentation under both load and displacement control. A power law fit to the initial unloading curve was used to determine a reduced elastic modulus for each material. Between 30 and 300 indentations were performed on each material, and ANOVA analysis was run to determine the statistical significance of differences in modulus between samples. Using nanoindentation, the 22 different samples had reduced modulus values ranging from 840 MPa to 4.14 GPa. Aspartic acid-methacrylate (Asp-MA) copolymers were not distinguishable from the pHEMA control material. Polymerization in the presence of HA created a more uniform material than the urea method of mineralization. Several challenges and solutions encountered in the nanomechanical testing of soft, heterogeneous materials are discussed. These results demonstrate that with proper experimental design, the mechanical properties of tissue engineering scaffold materials based on polymer-ceramic composite materials can be determined using small samples and nanoindentation techniques. © 2006 Wiley Periodicals, Inc. J Biomed Mater Res 81A: 611–623, 2007

Key words: tissue engineering; bone; pHEMA; nanoindentation; mechanical properties

INTRODUCTION

Materials characterization strategies for tissue engineering are of particular interest as more groups are taking combinatorial approaches toward screening.[1–3] Small amounts of materials that differ slightly from each other in composition are synthesized and tested for biocompatibility and specific biological function in a series of assays. The results of these screens often yield materials previously unknown to be biocompatible.[4] The ability to generate libraries of materials greatly outpaces our ability to test them mechanically. Small scale mechanical testing techniques, including nanoindentation and scanning force microscopy, are excellent techniques for this purpose. Using these techniques, several mechanical measurements can be made on small samples of each material in a library with minimal sample preparation, often nondestructively.

In previous work, one of us (J.S.) described the synthesis and characterization of a library of novel hydrogel scaffold materials for bone tissue engineering containing covalently bound anionic amino acid groups.[5] These materials are copolymers of 2-hydroxyethyl methacrylate (HEMA) and methacrylamides conjugated with anionic amino acids and their hydroxyapatite (HA) composites.[5,6] Anionic amino acids are known to act as nucleation sites for HA crystal formation *in vivo*.[7,8] To test the mineralization ability of these copolymer gels, the materials were mineralized with HA *in vitro*. The chemical composition, microstructure and crystallinity of the nucleated mineral in the hydrogel-HA composite has been previously analyzed using

Correspondence to: C. M. Klapperich; e-mail: catherin@bu.edu

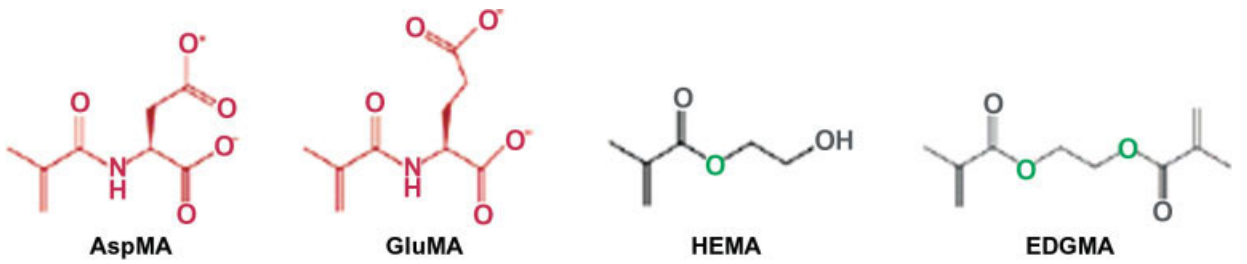

Figure 1. Schematic of AA-MA monomers. [Color figure can be viewed in the online issue, which is available at www.interscience.wiley.com.]

scanning electron microscopy (SEM), energy dispersive X-ray analysis and X-ray diffraction, and vary as a function of mineralization conditions.[6] In order to determine the potential success of these materials as bone tissue engineering scaffolds, it is necessary to gather data regarding their mechanical properties.

The anionic methacrylamide monomers are prone to premature polymerization and require chromatographic purification prior to copolymerization with HEMA. These difficulties require making the hydrogel copolymers in small quantities for preliminary testing. Further, by being able to test small amounts of each sample material, a library with wider breadth can be made using smaller amounts of the valuable comonomers. In this work we use instrumented indentation (nanoindentation) to perform mechanical tests on a library of copolymer materials incorporating a range of anionic monomer concentrations and a subset of these library materials after mineralization using two different *in vitro* mineralization methods.

Several investigators have used nanoindentation to determine the surface material properties of polymers,[9–11] and the technique has been used extensively to characterize bone and potential bone substitute materials.[12–16] The standard method for data analysis was described by Oliver and Pharr.[17] It was recognized early on that the time dependence of the mechanical properties of polymers complicated analysis of the indentation data.[18] Overestimation of the elastic modulus of polymers can occur due to creep effects and errors in determining the tip area function during calibration.[19,20] Experimental methods to correct for these errors have been widely applied. Trapezoidal loading curves are used in attempts to minimize creep effects on the initial unloading curve.[14] Others have developed methods for fitting the data during the hold period in a load control experiment to back out both the modulus values and time constants.[21] It is clear that the Oliver and Pharr method for computing a reduced elastic modulus from the initial unloading curve has its shortcomings, but for glassy polymers like the dehydrated pHEMA-based materials discussed here; the method is suitable for determining relative differences in surface mechanical behavior.

In the Oliver and Pharr method, the reduced elastic moduli of the samples are calculated using a power law fit to the initial unloading curve. The solution for an axisymmetric rigid indenter indenting on an elastic half space was presented by Sneddon[22] and elaborated by Oliver and Pharr.[17] From this solution, a simple equation for obtaining reduced modulus from a spherical indenter is obtained:

$$E_r = \frac{\sqrt{\pi}}{2\sqrt{A(h_c)}} S$$

where E_r is the reduced modulus, $A(h_c)$ is the area calculated as a function of contact depth, h_c, and S is the stiffness of the sample.

A conospherical indenter was chosen to minimize damage to the sample during testing. Several elastic solutions for spherical indenters have been previously derived,[20,23,24] and Bushby et al. developed specific methods for determining the area function of spherical indenters.[25,26] Nanoindentation with spherical tips has previously been used to analyze the mechanical properties of bone[14-16,27] and other HA composites.[13,28] Here we calibrate our tip by making serial indents at increasing depths in a polished polycarbonate sample of known elastic modulus as described in Klapperich et al.[29]

MATERIALS AND METHODS

Synthesis of monomers

The detailed synthesis and characterization of the anionic monomers is described in Song et al (Fig. 1).[6] Briefly, the amino acid-methacrylate monomer (AA-MA) was synthesized by reacting methacryloyl chloride with the amino acid under basic conditions. The amino acid was dissolved in water (with the addition of potassium hydroxide) and added to a tetrahydrofuran (THF) solution of methacryloyl chloride. The reaction was allowed to proceed at room temperature for 4 h while the pH was maintained at pH 8–9 by the addition of potassium hydroxide. After chromatography purification, spectroscopically (NMR and MS)

TABLE I
Description of Polymerization and Mineralization Conditions for the 22 pHEMA Samples Tested

Sample Name	Sample Description	Mineralization Conditions
Unmineralized Samples		
PH	pHEMA	Unmineralized control
A1	pHEMA-*co*-1%-Asp-MA	None
A2	pHEMA-*co*-2%-Asp-MA	None
A5	pHEMA-*co*-5%-Asp-MA	None
A10	pHEMA-*co*-10%-Asp-MA	None
A20	pHEMA-*co*-20%-Asp-MA	None
G1	pHEMA-*co*-1%-Glu-MA	None
G2	pHEMA-*co*-2%-Glu-MA	None
G5	pHEMA-*co*-5%-Glu-MA	None
G10	pHEMA-*co*-10%-Glu-MA	None
G20	pHEMA-*co*-20%-Glu-MA	None
Mineralization method 1 (polymerized in the presence of HA)		
PH_HA	pHEMA-HA	Polymerized in the presence of HA
A1_HA	pHEMA-*co*-1%-Asp-MA-HA	Polymerization occurred in the presence of HA suspension
A5_HA	pHEMA-*co*-5%-Asp-MA-HA	Polymerization occurred in the presence of HA suspension
A10_HA	pHEMA-*co*-10%-Asp-MA-HA	Polymerization occurred in the presence of HA suspension
G1_HA	pHEMA-*co*-1%-Glu-MA-HA	Polymerization occurred in the presence of HA suspension
G5_HA	pHEMA-*co*-5%-Glu-MA-HA	Polymerization occurred in the presence of HA suspension
G10_HA	pHEMA-*co*-10%-Glu-MA-HA	Polymerization occurred in the presence of HA suspension
Mineralization method 2 (urea-mediated mineralization)		
PH_UN	Hydrolyzed pHEMA, urea	Treated with the urea-mediated mineralization condition in the absence of HA
PH_Urea	pHEMA-HA, urea	Treated with the urea-mediated mineralization condition in the presence of HA
A5_Urea	pHEMA-*co*-5%-Asp-MA-HA, urea	Treated with the urea-mediated mineralization condition in the presence of HA
G5_Urea	pHEMA-*co*-5%-Glu-MA-HA, urea	Treated with the urea-mediated mineralization condition in the presence of HA

pure monomers were copolymerized with HEMA in the presence of 2 wt % of ethylene glycol dimethacrylate.

Copolymer preparation

To make a typical copolymer, 500 μg of a mixture of HEMA and the corresponding methacrylamide monomer were mixed with 10 μL of ethylene glycol dimethacrylate (EGDMA), which acts as a crosslinker. The components were diluted in 250 μL of a 2:3 Millipore water and ethylene glycol mixture, to which 50 μL each of an aqueous solution of sodium metabisulfite (150 mg/mL) and ammonium persulfate (400 mg/mL) were added to initiate the radical polymerization. Prior to gelling, radical inhibitors were removed from the commercial HEMA and EGDMA via distillation under reduced pressure and passing through a 4 Å molecular sieve column, respectively.

For this study, we used copolymers of HEMA and glutamic acid- and aspartic acid-conjugate methacrylamide (Glu-MA and Asp-MA), respectively. Copolymers containing 1, 2, 5, 10, and 20% of Asp-MA (sample names A1, A2, A5, A10, and A20) or Glu-MA (sample names G1, G2, G5, G10, or G20) were formed (Table I).

Mineralization method 1: Polymerization in the presence of HA

The first set of mineralized samples was made by performing the above polymerization and copolymer formation steps in the presence of HA powders (Alfa Aesar, Ward Hill, MA). The commercial HA powders are 1–10 μm agglomerates of polycrystalline HA about 100 nm in size. Before polymerization, the suspension of the HA particles was sonicated to break up the larger agglomer-

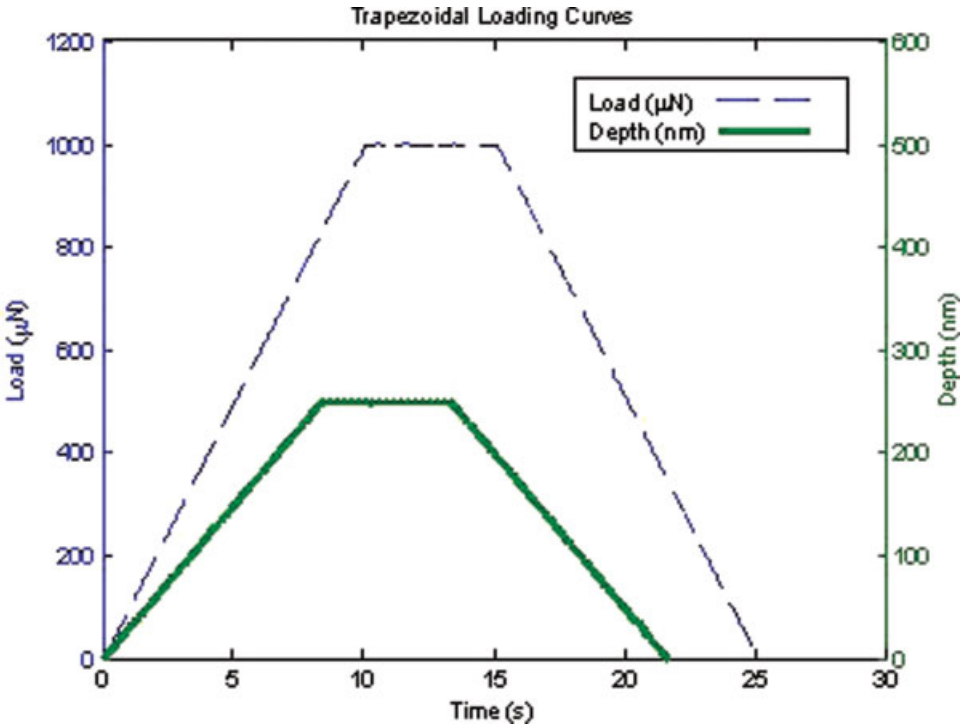

Figure 2. The trapezoidal loading curves used for load control (blue) and displacement control (green) experiments. Axis on the left shows load in microNewtons and axis on the right shows displacement in nanometers. [Color figure can be viewed in the online issue, which is available at www.interscience.wiley.com.]

ates. Copolymers containing only pHEMA, containing 1, 5, and 10% Asp-MA or containing 1, 5, and 10% Glu-MA were mineralized (sample names with _HA suffix in Table I).

Mineralization method 2: Urea-mediated HA mineralization

HA is insoluble in aqueous solutions at neutral and basic pH and soluble at acidic pH. A urea-mediated method[5,6] was used to generate copolymer-HA composite with robust mineral integration at the copolymer surface. In brief, HA (15 mg/mL) and 2*M* urea were dissolved in water at pH 2.5 at room temperature.[5,6] After adding the copolymers, the solution was heated from room temperature to 95°C at a constant heating rate of 0.2°C/min. The thermo-decomposition of urea led to the generation of ammonium, which gradually increased the pH of the mineral solution so that HA started to precipitate out. Meanwhile, the increase of pH and temperature also led to the *in situ* hydrolysis of the hydroxyethyl ester side chains of pHEMA, thereby generating abundant Ca^{2+}-binding surface carboxylates. The samples were heated for 10 h more upon reaching 95°C with a total mineralization time of ~16 h. The mineralized copolymers were thoroughly washed in Millipore water to remove loosely attached mineral precipitation. After rinsing, the composites were lyophilized before being tested with the nanoindenter. Copolymers containing only pHEMA, containing 5% Asp-MA or containing 5% Glu-MA were mineralized (sample names with _Urea suffix in Table I). A positive control sample (sample name PH_UN in Table I) was put through the urea-mediated mineralization method in the absence of HA in order to monitor any affects that the heat and pH changes have on the bulk properties of the polymer.

Nanoindentation

A Hysitron Triboscope Nanomechanical Test Instrument (Minneapolis, MN) was used to test the materials. The copolymer and composite samples from each treatment method were cut into small squares about 1-mm thick. After lyophilization, most samples were flat but had an uneven surface. Samples were attached to atomic force microscope (AFM) specimen discs with a thin layer of cyanoacrylate. Two types of experiments were performed on each sample. Load control indentations were made using a trapezoidal loading curve with a loading rate of 100 μN/s to a peak load of 1000 μN with a hold time of 5 s (Fig. 2). Displacement control indentations were made using a trapezoidal loading curve with a loading rate of 30 nm/s to a peak displacement of 250 nm with a hold time of 5 s (Fig. 2). The 20 μm conospherical diamond indenter was calibrated using optically polished polycarbonate (McMaster-Carr, Chicago, IL) with a known compressive modulus of 2.96 GPa.[30]

For both load and displacement control experiments, data were collected in real time. A reduced elastic modulus was subsequently calculated using a power law fit to the initial unloading curve for each indentation.[17] The values presented in the figures represent the mean and standard deviation of the successful indentations of the dry material. Successful indentations were defined as those

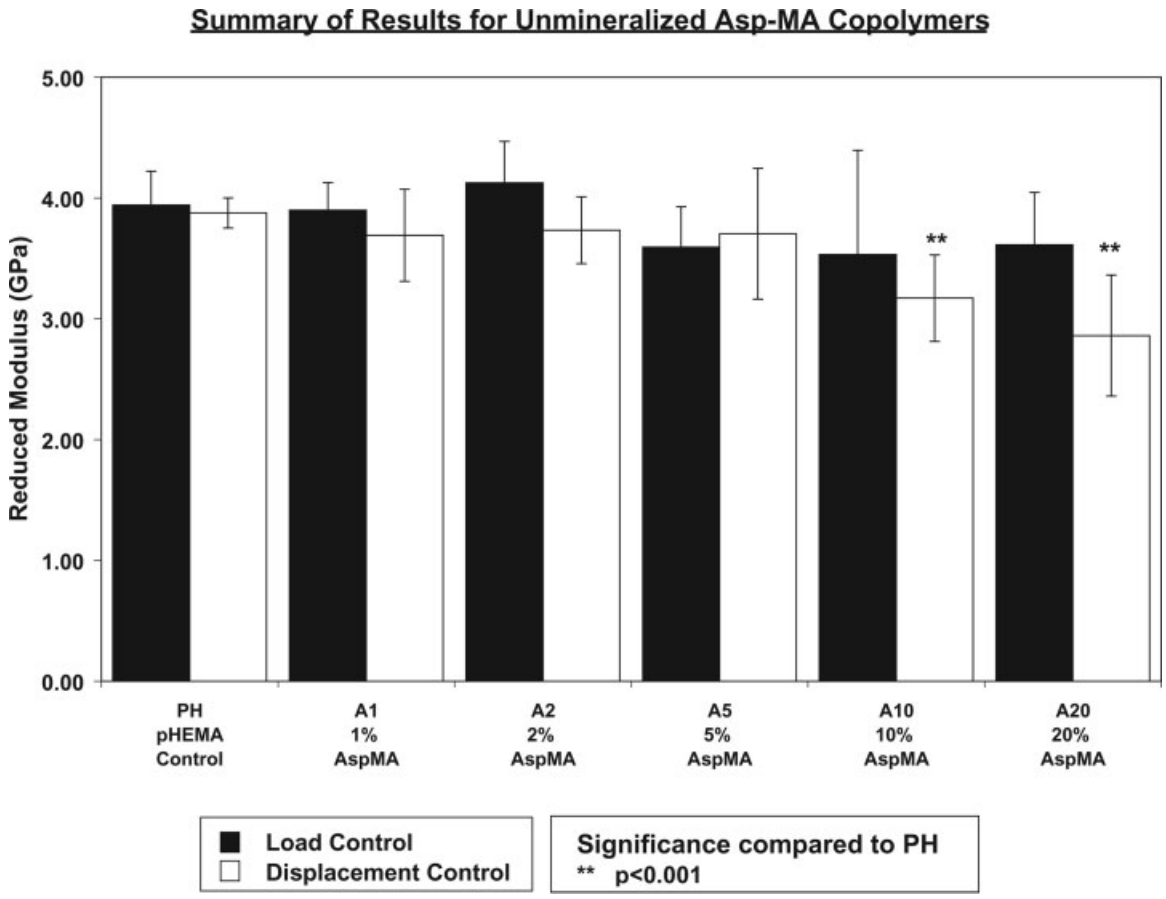

Figure 3. Results of nanoindentation experiments on unmineralized Asp-MA copolymers.

throughout which the computer was able to maintain load or displacement control. Occasionally the system would not maintain control or would fail to initially make complete contact with the surface resulting in data files containing random scatter. These indentations were eliminated from further analysis.

Data analysis

Thirty to 300 indentations were made on each sample in both load and displacement control using the trapezoidal load and displacement profiles shown in Figure 2. The load and displacement control results were considered separately since they represent measurements at different depths. To ensure that an indent was performed successfully, the standard deviation from an ideal loading curve was calculated. In load control indents, the actual load versus time curve was compared to the experimentally prescribed loading profile. In displacement control indents, the actual displacement versus time curve was compared to the experimentally prescribed displacement profile. The standard deviation of the actual load or displacement profile from all three segments of the ideal trapezoidal profile was computed for each indent. Indents with large standard deviations between the actual values and the ideal curves (above 1% for displacement control and 10% for load control) were eliminated from further analysis. The threshold for disqualification was lower for the displacement controlled indents because at very small standard deviation values the shape of the test curve was very different than what was initially requested by the user. Indents in which a visible fracture or other large change in loading slope occurred were also eliminated to correct for errors in the calculation of contact depth caused by incomplete contact during loading. This second type of error during nanoindentation was described in detail in Hayes et al.[10]

Statistical analysis

After elimination of failed indents, the reduced modulus values were calculated for each indentation. Load control and displacement control data for each sample were processed separately. The reduced modulus values for each sample were then read into the STATA statistical analysis program (StataCorp, College Station, TX). An analysis was performed using the STATA software to quantify the mean reduced modulus and standard deviation for each sample and determine significance. Significance was determined using a one-way analysis of variance with a Bonferroni multiple comparison test to examine the difference between each pair of means. P values of less than 0.05 were considered significant.

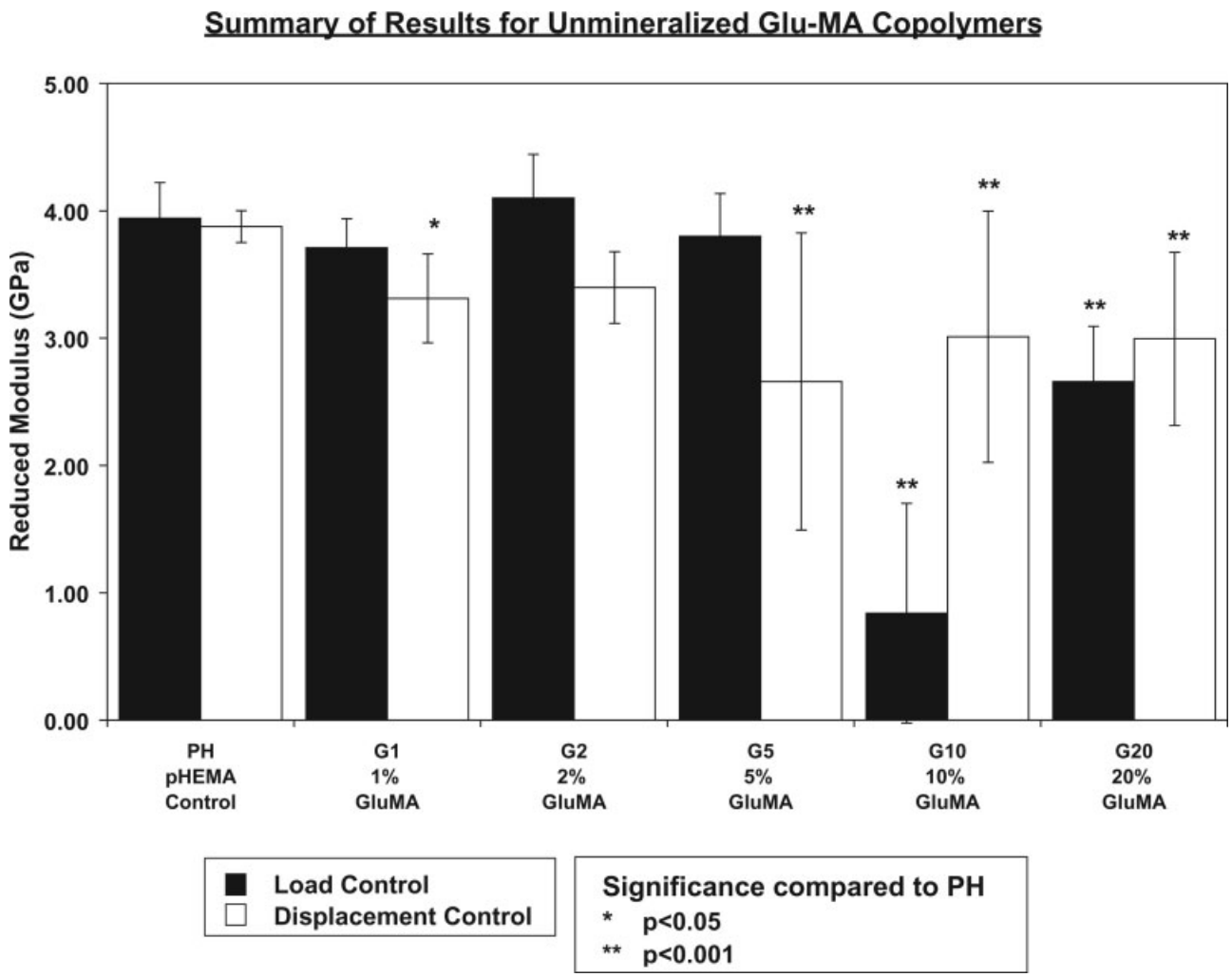

Figure 4. Results of nanoindentation experiments on unmineralized Glu-MA copolymers.

Scanning electron and atomic force microscopy

Scanning electron microscopy was used to get images of the surface microstructures of representative mineralized co-polymers. Several locations on representative samples were imaged using an AFM (MFP-3D, Asylum Research, Santa Barbara, CA) to determine a roughness average (R_a) on a size scale relevant to the tip-surface interaction area.

RESULTS

Table I lists the sample names and a short description of the processing conditions used to make each sample. The nanoindentation results for unmineralized Asp-MA copolymers are shown in Figure 3. The results for unmineralized Glu-MA copolymers are shown in Figure 4. The results for samples mineralized through polymerization in the presence of HA (method 1) are shown in Figure 5. The results for samples mineralized by the urea-mediated method (method 2) are shown in Figure 6. All modulus values are expressed as a reduced modulus, E_r, and are given in units of GPa. Samples that are significantly different from the unmineralized control, PH, are noted.

Displacement versus load control

The 22 samples were tested using both load and displacement control indentations. In most cases, the reduced moduli determined from fitting the displacement control indents do not differ significantly from the values determined using from load control indents. In the cases where they are significantly different, the displacement control modulus tends to be slightly lower. PH_Urea and G10 are exceptions to this trend. The overall trends present between samples hold whether the displacement control or load control moduli are used for comparison. Samples that showed a statistically significant disagreement between load and displacement control moduli are addressed individually in the Discussion.

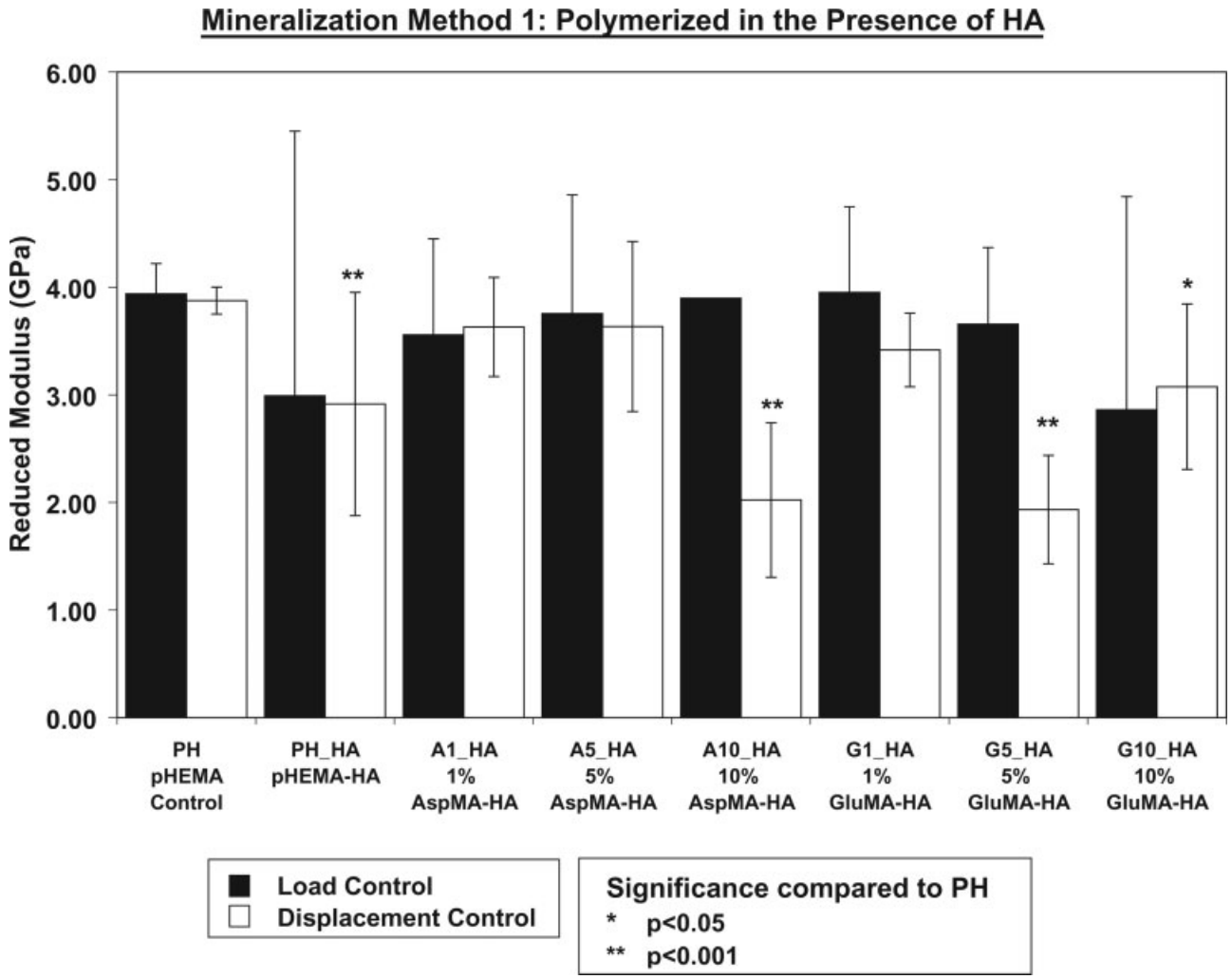

Figure 5. Results of nanoindentation experiments on samples mineralized through polymerization in the presence of HA.

Copolymerization of pHEMA with anionic comonomers

We looked at two classes of copolymers, those with glutamic acid (Glu-MA) conjugates and with aspartic acid (Asp-MA) conjugates. Overall, the addition of Glu-MA comonomer has more of an effect on the measured surface modulus than the addition of the Asp-MA comonomer. As the percentage of Asp-MA is increased, there is no change in the reduced modulus of the samples (Fig. 3) in the load control data. For the displacement controlled indents, only the highest percent Asp-MA copolymers, A10 and A20, show a decrease ($p < 0.001$) in reduced modulus compared to the PH control.

In both displacement and load control, increasing the percentage of Glu-MA decreases the reduced modulus of the sample (Fig. 4). The decrease is not monotonic, and the decrease is not consistent between load and displacement control measurements. As the percentage of Glu-MA is increased from 10 to 20% (G10 and G20), there is a decrease in the load control reduced elastic modulus ($p < 0.001$). In displacement control, there is a statistically significant difference as the percent monomer is increased from 2 to 5% (G2 and G5).

Mineralization method 1: Polymerization in the presence of HA

Samples mineralized by simply polymerizing the gel in the presence of HA (method 1) show no statistically significant reduction in the load control modulus compared to unmodified pHEMA (sample PH) (Fig. 5). The unmodified pHEMA polymerized in the presence of HA (PH_HA) has a lower displacement control reduced modulus ($p < 0.001$) than the unmineralized control. A10_HA, G5_HA, and G10_HA also all show a decrease ($p < 0.001$) in the displacement control modulus compared to the PH control.

Polymerization in the presence of HA had no statistically significant effect on the 5% Asp-MA/HEMA copolymer (A5_HA). Mineralization of the 5% Asp-MA/HEMA copolymers using the urea-mediated

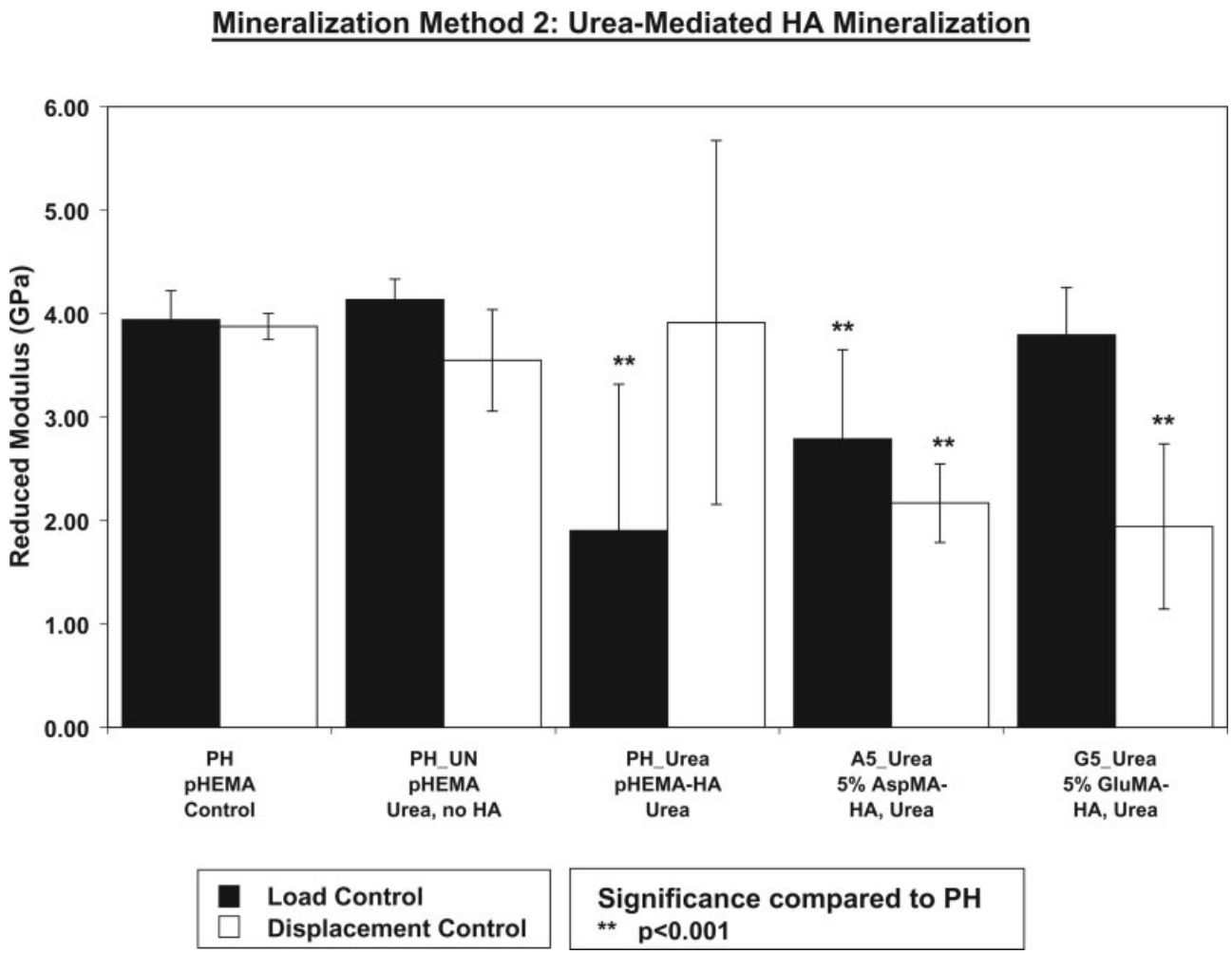

Figure 6. Results of nanoindentation experiments on samples mineralized using the urea-mediated mineralization method.

method led to a small decrease in displacement control modulus ($p < 0.05$) and no change in the load control modulus from the unmineralized 5% Asp-MA/HEMA copolymer (A5). Polymerization in the presence of HA of the 5% Glu-MA/HEMA copolymer (G5_HA) led to a small decrease in the displacement control reduced modulus ($p < 0.005$) compared to the unmineralized copolymer (G5).

Mineralization method 2: Urea-mediated mineralization

The sample treated with urea method in the absence of mineral, PH_UN, had the smallest decrease in modulus compared to the control. Recall that the PH_UN sample was run as a control to make sure that the urea-mediated method was not degrading the mechanical properties of the polymer itself. Copolymers mineralized via the urea method showed a decrease ($p < 0.001$) in the displacement control reduced moduli when compared to the unmodified pHEMA (PH) (Fig. 6). A5_Urea showed decreases ($p < 0.001$) in the load and displacement control moduli measurements compared to the control, PH. Only the displacement control modulus was lower in the G5_Urea sample. Although the average moduli of PH and PH_Urea were similar in displacement control, the standard deviations of the moduli of PH_Urea increased from 3 to 45% of the mean.

Topology of mineralized copolymers

SEM of the materials mineralized by the different methods shows significant differences in surface topology (Fig. 8). The samples mineralized by the urea method have large areas of mineral surrounded by unmineralized areas [Figs. 8(A–C)]. The samples polymerized in the presence of HA have a much smoother appearance and do not exhibit surface heterogeneity on the size scale of SEM [Figs. 8(D,E)]. The nanoindentation data reflect these differences in the standard deviations about the mean of all indentations made on a particular sample. Samples with

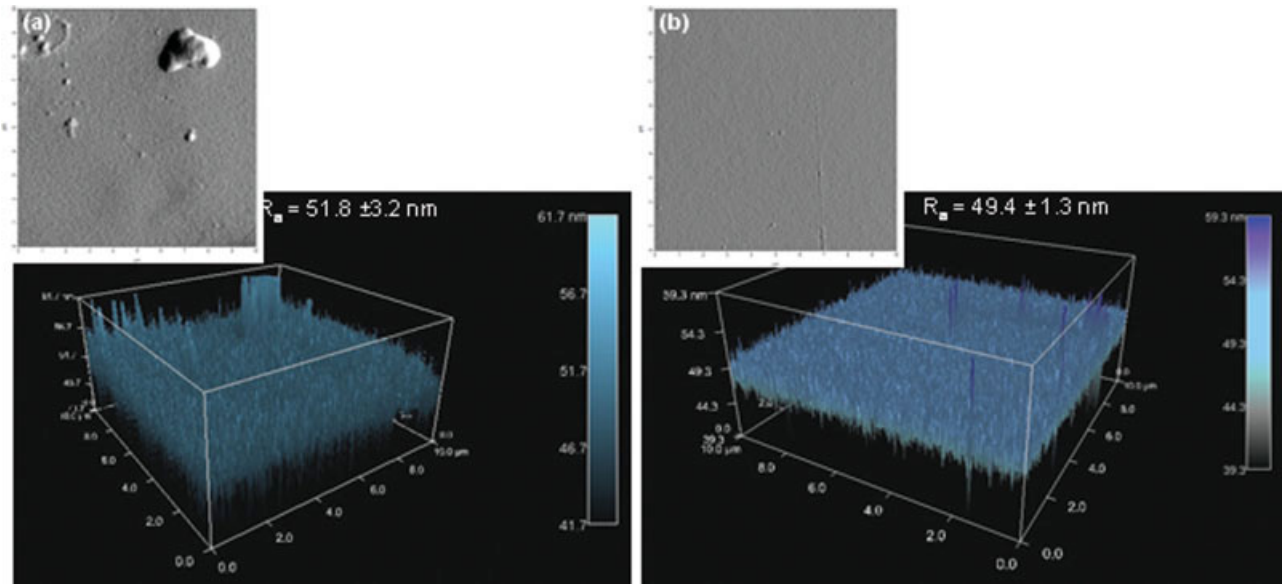

Figure 7. AFM images of surface roughness of two representative samples (a) A5_Urea, a urea mineralized sample and (b) A5_HA, a sample mineralized in the presence of HA particles. Insets are images looking from the top down. [Color figure can be viewed in the online issue, which is available at www.interscience.wiley.com.]

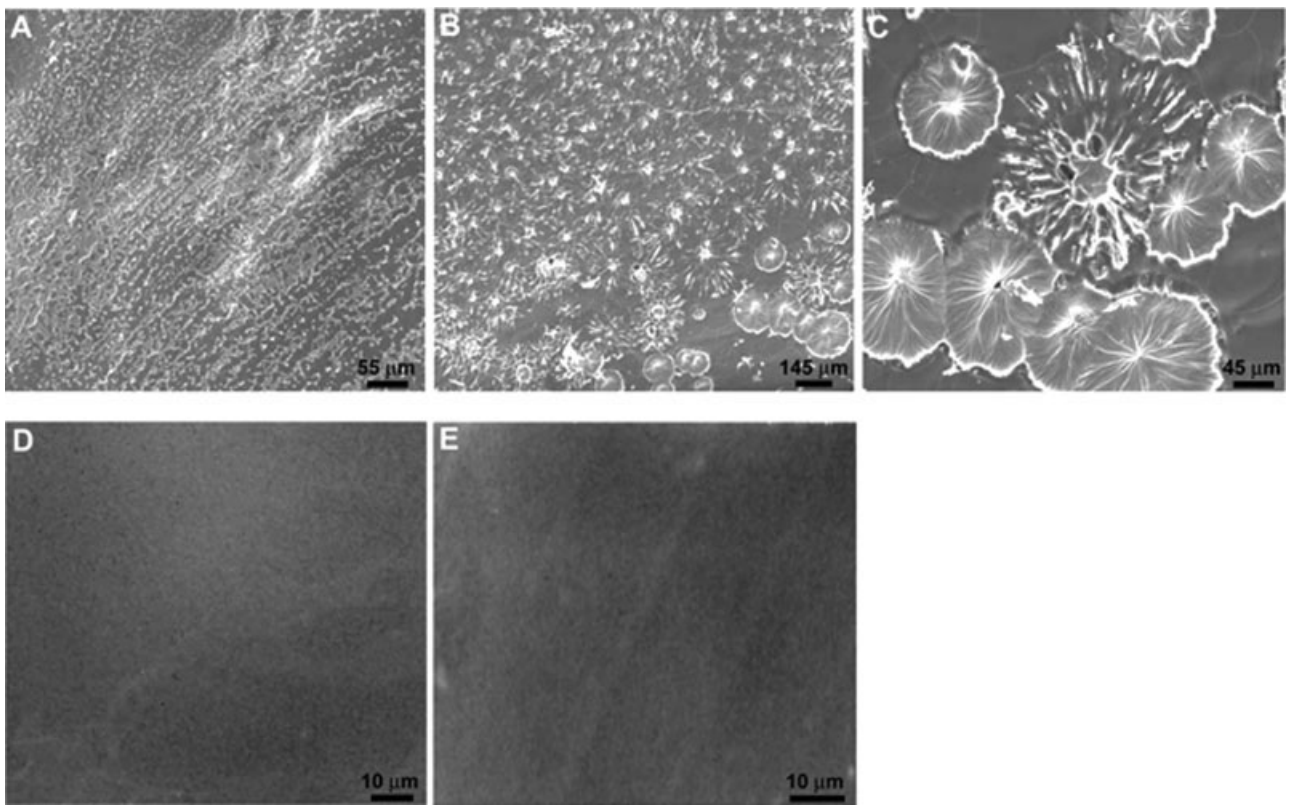

Figure 8. SEM micrographs of HA-mineralized pHEMA-based hydrogels functionalized with 5 wt % of anionic amino acid residues. (A) and (B) p(HEMA-*co*-5%Asp-MA)-HA and p(HEMA-*co*-5%Glu-MA)-HA composites, respectively, obtained by the urea-mediated HA-mineralization (room temperature to 95°C, 0.2°C/min). Note that the formation of white mineral domains across the surface of the hydrogel copolymer (darker background). (C) A zoom-in view of micrograph B. Note the merging of circular mineral domains. (D) & (E) p(HEMA-*co*-5%Asp-MA)-HA and p(HEMA-*co*-5%Glu-MA)-HA composites, respectively, obtained by copolymerizing hydrogel monomers in the presence of HA suspensions at room temperature. Note the smooth surface appearance of the composite, suggesting a uniform distribution of HA nano-sized particles throughout the hydrogel scaffold.

more microscale topography have larger standard deviations.

Since the area of tip-sample interaction is smaller than these observed microscale features, we performed AFM scans on 10 μm × 10 μm areas on representative samples mineralized by the two methods. One of the samples was mineralized using the urea method, A5_Urea [Fig. 7(a)] and the other was polymerized in the presence of HA, A5_HA [Fig. 7(b)]. Surface roughness values were calculated for the 10 μm square area by the AFM software. The results at this size scale were similar for both surfaces; R_a= 51.8 ± 3.2 nm and 49.4 ± 1.3 nm, respectively.

DISCUSSION

Displacement versus load control

When samples are tested in load control, the transducer modulates the electrostatic force to compensate for the stiffness of the sample and maintain a constant applied force during the test.[31] A softer sample will undergo more displacement in the z-direction than a stiffer sample at the same applied load. The result is that indents performed at the same maximum load will not necessarily probe the same depth of a sample when different materials are compared or more than one location on the same sample is tested. In the event that the mechanical properties vary as a function of penetration depth, it may be difficult to see this variation between samples when comparing load controlled indents.

When samples are tested in displacement control, the sample is indented to the same depth each time, here to a depth of 250 nm. In displacement control, the mechanical properties of different materials are compared at the same sampling depth. It is significantly more difficult to maintain contact with the sample in displacement control than in load control because the Hysitron TriboScope is nominally force controlled. These differences must be kept in mind when comparing the mechanical properties of samples determined using each method. It is not surprising that displacement control indents at depth of 250 nm and load control indents at depths up to 2 μm will yield different results. Specifically, if a sample has a surface layer that is either softer or stiffer than the bulk, this effect will be seen more acutely in the displacement controlled indents.

Copolymerization of pHEMA with anionic comonomers

The addition of the conjugated monomers was not expected to significantly change the polymer mechanical properties, since the size of the conjugated amino acids is small, and the polymer backbone should remain unchanged for similar polymerization conditions and crosslinking amounts. In general, the Asp-MA/HEMA copolymers behaved as expected and maintained fairly constant reduced modulus values that were similar in both load and displacement control, indicating that the surface and the material had homogeneous mechanical properties throughout (Fig. 3). The Glu-MA/HEMA copolymers showed a decreasing modulus with increasing Glu-MA percentage (Fig. 4).

The decrease in the reduced modulus in the Glu-MA/HEMA copolymers may be due to phase separation of the monomers during or after polymerization. When the percentage of negatively charged glutamic acid residues increases, the role of electrostatic repulsion may become more significant and could affect the efficiency of the polymerization and crosslinking. The additional methyl group in the glutamic acid side group may be responsible for a difference in solubility between the two monomers. This hypothesis is supported by the increase in measurement variance at high Glu-MA concentrations. Increased variance in measured properties is a result of surface heterogeneity, which could occur as a result of phase separation or incomplete polymerization. Which mechanism is at work is still under investigation.

The lower percentage Asp-MA gels (A1, A2, and A5) showed no significant difference in modulus from the unmodified control material. A10 and A20 had similar load control moduli to unmodified pHEMA, but had significantly lower displacement control moduli. The high percentages of Asp-MA monomer likely lead to the differences between the surface and bulk because of incomplete solubility leading to surface segregation or phase separation of the monomer at this high concentration. Since aspartic and glutamic acid structures are identical except for the additional methyl group on the glutamic acid side chain, it would follow that both monomers would show similar solubility effects. It is expected that the aspartic acid monomer would show these effects at a higher percentage of monomer and be less pronounced, since the monomer is smaller and more soluble.

Mineralization methods

There was some concern that the urea-mediated mineralization method (method 2) would degrade the mechanical properties of the underlying copolymer due to the high temperature and low pH conditions that leads to partial hydrolysis of the hydroxyethyl ester side chains and/or the ester-based crosslinkers. We did observe that all samples treated with

this method showed a decrease in either the displacement control or load control reduced modulus when compared to the unmodified pHEMA sample, PH. There was a marked change in the behavior of the PH_Urea gel modified by the urea-mediated mineralization compared to the control. The large standard deviation and decrease in average modulus in the load control modulus of PH_Urea may represent polymer degradation and mineralization occurring simultaneously. Interestingly, we did not see a degradation of the mechanical properties when the urea treatment was performed on plain pHEMA in the absence of HA particles, suggesting that the concentration of ions in the solution may play a role in degradation of the underlying copolymer.

In general, the samples polymerized in the presence of HA are not significantly different from the control samples. None of the load control moduli for the gels polymerized in the presence of HA are significantly different from the unmodified control, PH. A few samples, PH_HA, A10_HA, G5_HA, and G10_HA, have significantly lower displacement control moduli than PH (Fig. 5). Again, the lower modulus values are measured in displacement control at the relatively shallow fixed maximum displacement of 250 nm indicating a true surface softening effect. We speculate that segregation of the HA particles near the surface may locally inhibit polymerization and lead to lower local molecular weight.

For both methods, we expected that the mineralized samples would be stiffer than the unmineralized control, since the elastic modulus of HA has been reported in the range of 40–150 GPa depending on the processing conditions used to make the particles and how dense the particles are after processing.[32–34] A weaker matrix phase resulting from composite processing may explain some of the discrepancy. A simple rule of mixtures calculation predicts that addition of the HA particles will increase the composite reduced elastic modulus. It is likely that the HA formed on the urea-mediated samples is less dense and amorphous or nanocrystalline,[5] so it does not have the same mechanical stiffness as the larger HA particles. Additionally, if the HA phase is porous, it will fracture or crumble under the force of the tip and appear to be less stiff than a full sintered particle.

In the case of copolymers containing Asp-MA or Glu-MA, it is not known if all of the HA particles in suspension were incorporated into the composites. The HA particles likely are "dissolved" by the acidic environment of the Asp and Glu residues resulting in a more homogeneous composite material. This phenomenon may explain why the images in Figures 8(D,E) lack any significant topology after mineralization even though energy dispersive X-ray analysis has demonstrated the presence of HA.[5]

Comparison to bone

The load control and displacement control reduced moduli determined for this new class of bone mimics range from 840 MPa to 4.13 GPa. The elastic modulus along the length of a human femur measured using nanoindentation was found to be between 6.9 and 25.0 GPa.[14,27,35,36] The lower modulus of these composite materials is not expected to inhibit the eventual repair of bone defects, since the calculated moduli are similar to the reported elastic modulus range of trabecular bone.[37] The intended end use of these materials is as a scaffold to induce osteoblast ingrowth and mineralization activity in the body. This application requires that the scaffold be mechanically robust, but it does not require that the initial implanted scaffold match the mechanical properties of the eventual desired tissue replacement. A successful scaffold will be one that can stimulate new bone synthesis via mechanical and chemical signals, which does not necessarily require an initial stiffness matching healthy bone.

Comments on time dependence

In this study, we did not consider the time-dependent properties of the copolymers under investigation. Although we are confident that the values obtained are in the appropriate order of magnitude and that the relative changes are real, it is important to note that in biomaterials and soft tissues, these effects must be taken into account when attempting to determine true (not relative) mechanical properties. The primary concern when using the initial unloading curve to determine the stiffness of glassy polymers is that the unloading rate may be slower than the creep rate. If this is the case, the unloading curve will bow out, resulting in overestimation of the material stiffness. In order to ameliorate this problem here, we have added in a hold period during which most of the material creep will take place. By the time the unloading point is reached, the creep rate will be slower than the unloading rate. The effect can be seen in both load and displacement control, so we have incorporated the hold period in each case. The unloading rate for the displacement controlled experiments was -406 μN/s, while the final stress relaxation rate (measured at the end of the hold period) was -17.6 μN/s. The unloading rate for our load control indents was -2.76 nm/s, while the final creep rate was 1.40 nm/s. Since the mechanical properties of polymers are dependent on strain rate, it is important that strain rates be constant between tests comparing two different materials.[38] To determine time dependent properties, it is necessary to perform creep or stress relaxation tests

by using longer hold periods and fitting the hold period force-displacement behavior to an appropriate model. Several groups have recently published in this area.[20,39,40]

Nanoindentation for evaluation of new biomaterials

Nanoindentation can provide useful information when screening novel biomaterials for mechanical performance. Due to the many sources of error present when testing soft materials, it is imperative that a statistically relevant number of indentations be made to assure that only significant differences in mechanical properties between samples are detected. More indentations are often required on heterogeneous surfaces to insure that a minimum number of successful indents are completed and all regions of a material are tested. A limitation of this study is the use of the Oliver-Pharr method to measure the stiffness of the glassy polymer samples. In order to get true mechanical properties that can be compared with bulk values (rather than relative measurements), a time-dependent analysis should be done using creep and stress relaxation experiments.

Nanoindentation of pHEMA derived bone mimics has shown that mechanical testing can be used to measure the surface mechanical properties of libraries of biomaterials that are initially available only in small amounts. In past work, we have demonstrated that indentation of various thermoplastic polymers yields reduced elastic moduli in close agreement with bulk values obtained using macroscale methods[29] and that some surface modifications of thermoplastics can be detected using nanoindentation.[29,41] We can infer from that work that the values obtained in this study are reasonably correlated to what bulk properties of uniform copolymers and the surface properties of the urea-treated copolymers that would be obtained if these materials were available for bulk testing.

Challenges remain in relating the results of nanoindentation of polymers to the bulk properties of new polymers and composites. Van Landingham et al. provide a detailed review of the specific challenges of applying traditional load-displacement analyses to polymeric materials.[11] In particular, new fitting techniques will need to be selected for testing these materials in a hydrated state to account for the highly nonlinear behavior that is observed.

References

1. Simon CG Jr, Eidelman N, Kennedy SB, Sehgal A, Khatri CA, Washburn NR. Combinatorial screening of cell proliferation on poly(L-lactic acid)/poly(D,L-lactic acid) blends. Biomaterials 2005;26:6906–6915.
2. Kohn J. New approaches to biomaterials design. Nat Mater 2004;3:745–747.
3. Hubbell JA. Biomaterials science and high-throughput screening. Nat Biotechnol 2004;22:828,829.
4. Anderson DG, Levenberg S, Langer R. Nanoliter-scale synthesis of arrayed biomaterials and application to human embryonic stem cells. Nat Biotechnol 2004;22:863–866.
5. Song J, Malathong V, Bertozzi CR. Mineralization of synthetic polymer scaffolds: A bottom-up approach for the development of artificial bone. J Am Chem Soc 2005;127:3366–3372.
6. Song J, Saiz E, Bertozzi CR. A new approach to mineralization of biocompatible hydrogel scaffolds: An efficient process toward 3-dimensional bonelike composites. J Am Chem Soc 2003; 125:1236–1243.
7. Boskey AL. Mineral-matrix interactions in bone and cartilage. Clin Orthop Relat Res 1992:244–274.
8. Huq NL, Cross KJ, Ung M, Reynolds EC. A review of protein structure and gene organisation for proteins associated with mineralised tissue and calcium phosphate stabilisation encoded on human chromosome 4. Arch Oral Biol 2005;50: 599–609.
9. Briscoe BJ, Fiori L, Pelillo E. Nano-indentation of polymeric surfaces. J Phys D Appl Phys 1998;31:2395–2405.
10. Hayes SA, Goruppa AA, Jones FR. Dynamic nanoindentation as a tool for examination of polymeric materials. J Mater Res 2004;19:3298–3306.
11. VanLandingham MR, Villarrubia JS, Guthrie WF, Meyers GF. Nanoindentation of polymers: An overview. Macromol Symp 2001;167:15–44.
12. Tai K, Qi HJ, Ortiz C. Effect of mineral content on the nanoindentation properties and nanoscale deformation mechanisms of bovine tibial cortical bone. J Mater Sci Mater Med 2005;16:947–959.
13. Chowdhury S, Thomas V, Dean D, Catledge SA, Vohra YK. Nanoindentation on porous bioceramic scaffolds for bone tissue engineering. J Nanosci Nanotechnol 2005;5:1816–1820.
14. Bushby AJ, Ferguson VL, Boyde A. Nanoindentation of bone: Comparison of specimens tested in liquid and embedded in polymethylmethacrylate. J Mater Res 2004;19:249–259.
15. Zysset PK, Guo XE, Hoffler CE, Moore KE, Goldstein SA. Mechanical properties of human trabecular bone lamellae quantified by nanoindentation. Technol Health Care 1998;6 429–432.
16. Rho JY, Tsui TY, Pharr GM. Elastic properties of human cortical and trabecular lamellar bone measured by nanoindentation. Biomaterials 1997;18:1325–1330.
17. Oliver WC, Pharr GM. Improved technique for determining hardness and elastic modulus using load and displacement sensing indentation experiments. J Mater Res 1992;7:1564–1580.
18. Oyen ML, Cook RF. Load-displacement behavior during sharp indentation of viscous-elastic-plastic materials. J Mater Res 2003;18:139.
19. Tang B, Ngan AHW. Accurate measurement of tip-sample contact size during nanoindentation of viscoelastic materials. J Mater Res 2003;18:1141–1148.
20. Oyen ML. Spherical indentation creep following ramp loading. J Mater Res 2005;20:2094–2100.
21. Ngan AHW, Tang B. Viscoelastic effects during unloading in depth sensing indentation. J Mater Res 2002;17:2604–2610.
22. Sneddon IN. The relation between load and penetration in the axisymmetric Boussinesq problem for a punch of arbitrary profile. Int J Eng Sci 1965;3:47–57.
23. Field JS, Swain MV. Simple predictive model for spherical indentation. J Mater Res 1993;8:297–306.
24. Cheng L, Xia X, Scriven LE, Gerberich WW. Spherical-tip indentation of viscoelastic material. Mech Mater 2005;37:213–226.

25. Bushby A. Nano-indentation using spherical indenters. Nondestruct Test Eval 2001;17:213–234.
26. Bushby AJ, Jennett NM. Determining the area function of spherical indenters for nanoindentation. In: Materials Research Society Symposium—Proceedings. Boston, MA: Materials Research Society; 2001. pp 7–17. Materials Research Society Symposium—Proceedings.
27. Rho JY, Roy ME II, Tsui TY, Pharr GM. Elastic properties of microstructural components of human bone tissue as measured by nanoindentation. J Biomed Mater Res 1999;45:48–54.
28. Pelled G, Tai K, Sheyn D, Zilberman Y, Kumbar S, Nair LS, Laurencin CT, Gazit D, Ortiz C. Structural and nanoindentation studies of stem cell-based tissue-engineered bone. J Biomech 2006.
29. Klapperich C, Komvopoulos K, Pruitt L. Nanomechanical properties of polymers determined from nanoindentation experiments. J Tribol Trans ASME 2001;123:624–631.
30. L. Pruitt DR. The effect of specimen thickness and stress ratio on the fatigue behavior of polycarbonate. Polym Eng Sci 1996;36: 1300–1305.
31. Warren OL, Downs SA, Wyrobek TJ. Challenges and interesting observations associated with feedback-controlled nanoindentation. Z Metallkd 2004;95:287–296.
32. Katz JL. Hard tissue as a composite material. I. Bounds on the elastic behavior. J Biomech 1971;4:455–473.
33. Katz JL, Ukraincik K. On the anisotropic elastic properties of hydroxyapatite. J Biomech 1971;4:221–227.
34. Gardner TN, Elliott JC, Sklar Z, Briggs GAD. Acoutsic microscope study of the elastic properties of fluorapatite and hydroxyapatite, tooth enamel and bone. J Biomech 1992;25:1265–1277.
35. Zysset PK, Edward Guo X, Edward Hoffler C, Moore KE, Goldstein SA. Elastic modulus and hardness of cortical and trabecular bone lamellae measured by nanoindentation in the human femur. J Biomech 1999;32:1005–1012.
36. Oyen ML, Ko C-C, Bembey AK, Bushby AJ, Boyde A. Nanoindentation and finite element analysis of resin-embedded bone samples as a three-phase composite material. Materials Research Society Symposium Proceedings. San Francisco, CA: Materials Research Society; 2005. Warrendale, PA 15086, United States. pp 85–90. Materials Research Society Symposium Proceedings.
37. Keaveny TM, Morgan EF, Niebur GL, Yeh OC. Biomechanics of trabecular bone. Annu Rev Biomed Eng 2001;3:307–333.
38. Fujisawa N, Swain M. Effect of unloading strain rate on the elastic modulus of a viscoelastic solid determined by nanoindentation. J Mater Res 2006;21:708–714.
39. Yang S, Zhang Y-W, Zeng K. Analysis of nanoindentation creep for polymeric materials. J Appl Phys 2004;95:3655–3666.
40. Sakai M. Time-dependent viscoelastic relation between load and penetration for an axisymmetric indenter. Philos Mag A 2002;82:1841–1849.
41. Klapperich C, Pruitt L, Komvopoulos K. Nanomechanical properties of energetically treated polyethylene surfaces. J Mater Res 2002;17:423–430.